

## **Distribution Agreement**

In presenting this thesis as a partial fulfillment of the requirements for a degree from Emory University, I hereby grant to Emory University and its agents the non-exclusive license to archive, make accessible, and display my thesis in whole or in part in all forms of media, now or hereafter known, including display on the world wide web. I understand that I may select some access restrictions as part of the online submission of this thesis. I retain all ownership rights to the copyright of the thesis. I also retain the right to use in future works (such as articles or books) all or part of this thesis.

Signature:

---

BenMaan I. Jawdat

---

04-12-2010

**Characterization of the Interaction of Photo-Generated Cob(I)inamide with  
Carbon Dioxide in Anaerobic Aqueous Solution**

by

BenMaan I. Jawdat

Adviser: Dr. Kurt Warncke, Ph.D.

Department of Physics

---

Dr. Kurt Warncke, Ph.D.  
Adviser

---

Dr. Vincent Huynh, Ph.D.  
Committee Member

---

Dr. Cora MacBeth, Ph.D.  
Committee Member

---

04-12-2010

**Characterization of the Interaction of Photo-Generated Cob(I)inamide with  
Carbon Dioxide in Anaerobic Aqueous Solution**

By

BenMaan I. Jawdat

Adviser: Dr. Kurt Warncke, PhD.

An abstract of  
A thesis submitted to the Faculty of Emory College of Arts and Sciences  
of Emory University in partial fulfillment  
of the requirements of the degree of  
Bachelor of Arts with Honors

Department of Physics

2010

## Abstract

### **Characterization of the Interaction of Photo-Generated Cob(I)inamide with Carbon Dioxide in Anaerobic Aqueous Solution**

By BenMaan I. Jawdat

One of the greatest challenges facing today's scientists is the creation of a viable renewable energy system to meet the demands of a growing population. The use of solar energy is currently a research focus. The long-term goal of this project is to develop a light-driven catalytic module in a re-engineered protein, that will be used for conversion of carbon dioxide ( $\text{CO}_2$ ) to a stable fuel in aqueous solution. The selected protein is the EutB protein from ethanolamine ammonia-lyase, which contains the native, cobalt-containing cobalamin cofactor. In this project, the reactivity of the free cobinamide (modified cobalamin) molecule with  $\text{CO}_2$  is studied in buffered aqueous solution, outside of the protein environment. Static and time-resolved ultraviolet (UV)/visible spectroscopy is used to characterize the cobinamide in the absence and presence of  $\text{CO}_2$ . The fully-reduced cob(I)inamide, was generated by photoreduction of methylcob(III)inamide with 5'-deazariboflavin/EDTA in anaerobic, buffered (pH=6.0) solution. The subsequent cob(I)inamide decay reaction was measured by the loss of absorbance at 387 nm, with and without  $\text{CO}_2$  in solution. An assay was developed, in which the photolysis of methylcobalamin, and the subsequent reaction of the cob(II)alamin photoproduct with oxygen ( $\text{O}_2$ ) to form AquoCbl, was used to quantify the oxygen content in the samples. The careful control of pH and exclusion of oxygen led to dramatic improvement in the reproducibility of the cob(I)inamide reaction measurements, relative to previous attempts. Decay of cob(I)inamide in the absence of  $\text{CO}_2$  ( $\tau=9.0$  min) was assigned to a proton reduction reaction. Increased time constants for decay of cob(I)inamide (up to  $\tau=13.5$  min) were observed in the presence of  $\text{CO}_2$ . We propose that the effect is caused by the interaction of  $\text{CO}_2$  with cob(I)inamide.

**Characterization of the Interaction of Photo-Generated Cob(I)inamide with  
Carbon Dioxide in Anaerobic Aqueous Solution**

by

BenMaan I. Jawdat

Adviser: Dr. Kurt Warncke, Ph.D.

A thesis submitted to the Faculty of Emory College  
of Emory University in partial fulfillment  
of the requirements of the degree of  
Bachelor of Arts with Honors

Department of Physics

2010

## Table of Contents

| Chapter |   | Page |
|---------|---|------|
| I.      | Introduction  | 1    |
| II.     | Experimental Procedures   | 5    |
|         | - Absorption Spectroscopy   | 5    |
|         | - Photolysis Studies  | 5    |
|         | - Preparation of MeCbi Samples  | 6    |
|         | - Fitting of the Cob(I)inamide Decay Kinetics   | 8    |
| III.    | Results   | 9    |
|         | - Absorption Spectra of Different Cobalamin and Cobinamide Redox States   | 9    |
|         | - Assay for the Determination of Oxygen Concentration in the Samples  | 11   |
|         | - Reaction of Cob(I)inamide in Aqueous Solution at pH 6.0   | 14   |
|         | - Reaction of Cob(I)inamide with CO <sub>2</sub> in Aqueous Solution at pH 6.0  | 15   |
| IV.     | Discussion  | 20   |
|         | - Establishment of Reliability and Reproducibility in Cobalamin/ Cobinamide – CO <sub>2</sub> Reactivity Measurements | 20   |
|         | - Dihydrogen Formation  | 21   |
|         | - CO <sub>2</sub> Binding Interaction with Cob(I)inamide  | 22   |
|         | - Future Experiments and Outlook  | 23   |
| V.      | References  | 25   |

## List of Figures and Tables

| Figure |   | Page |
|--------|---|------|
| 1      | Top view of the ( $\beta\alpha$ ) <sub>8</sub> TIM-barrel   | 2    |
| 2      | Structure of cobalamin cofactors  | 3    |
| 3      | Coordination of cobalt oxidation states   | 3    |
| 4      | Target reaction between cob(I)alamin and CO <sub>2</sub> , in the active site of EutB   | 4    |
| 5      | UV/visible absorption spectra of cobalamin compounds in aqueous solution at room temperature  | 10   |
| 6      | UV/visible absorption spectra of cobinamide compounds in aqueous solution at room temperature   | 10   |
| 7      | Ultraviolet/visible spectra of MeCbl and photolysis to Cbl(II) without bicarbonate added, Ultraviolet/visible spectra of MeCbl and photolysis to Cbl(II) with bicarbonate added | 13   |
| 8      | Reaction of photo-generated cob(I)inamide in aqueous solution at pH 6.0   | 15   |
| 9      | Reaction of photo-generated cob(I)inamide in aqueous solution at pH 6.0 in the presence of different concentrations of bicarbonate  | 16   |
| 10     | Original data from Trial 2 of the 50 mM bicarbonate experiment, with the exponential fit curve overlaid   | 17   |
| 11     | Binding of CO <sub>2</sub> to the Co(I) complex in cob(I)inamide  | 21   |

| <b>Table</b>   | <b>Page</b> |
|--|-------------|
| 1 Monoexponential fit constants for the data of Figure 8 and 9 | 18          |

### List of Abbreviations

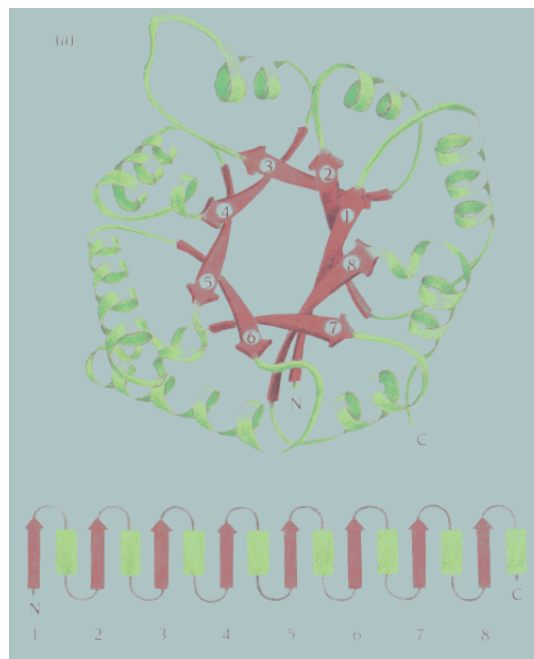
|  |                    |
|--|--------------------|
| Nicotinamide adenine dinucleotide phosphate  | (NADPH)            |
| Ribulose biphosphate carboxylase oxygenase   | (RUBISCO)          |
| Ethanolamine ammonia lyase                   | (EAL)              |
| Carbon dioxide                               | (CO <sub>2</sub> ) |
| Dimethylbenzimidazole                        | (DMB)              |
| Ultraviolet                                  | (UV)               |
| Dinitrogen                                   | (N <sub>2</sub> )  |
| Methylcobinamide                             | (MeCbi)            |
| Methylcobalamin                              | (MeCbl)            |
| 2-( <i>N</i> -morpholino)ethanesulfonic acid | (MES)              |
| Ethylenediaminetetraacetic acid              | (EDTA)             |
| 5'-Deazariboflavin                           | (5'DRF)            |
| Aquocobalamin                                | (AquoCbl)          |
| Aquocobinamide                               | (AquoCbi)          |
| Dioxygen                                     | (O <sub>2</sub> )  |
| Carbon monoxide                              | (CO)               |
| Dihydrogen                                   | (H <sub>2</sub> )  |
| Infrared                                     | (IR)               |

## I. Introduction

One of the greatest challenges facing today's scientists is the creation of a viable renewable energy system to meet the demands of a growing population. The use of solar energy as an energy source is currently a focus of research, because of its abundance; it powers all of life on earth using a fraction of the sun's energy. The key to be able to harness this energy would be to convert it into the form of "solar fuels", which could be stored and used day or night to meet our energy needs.<sup>1,2</sup> In nature, plants and bacteria have their own mechanisms for converting the sun's energy into chemical energy that they can use to grow. In plants, for example, the reaction is split into light and dark reactions; water is oxidized to extract an electron that goes on to make nicotinamide adenine dinucleotide phosphate (NADPH), which is used in the dark reactions to reduce carbon dioxide. The enzyme used in this system to reduce carbon dioxide, ribulose biphosphate carboxylase oxygenase (RUBISCO),<sup>3</sup> is neither efficient (slow turnover rate) nor specific (dioxygen and carbon dioxide have comparable affinities);<sup>4</sup> in addition, the reactions must be separated in space and in time in order to work in the environment of the organism. These rate limitations and inefficiencies of spatial and temporal separation could be circumvented by engineering a new, single protein that could carry out the light initiated charge separation as well as the reduction reaction. This type of modular molecular system is termed "compressed photosynthesis."

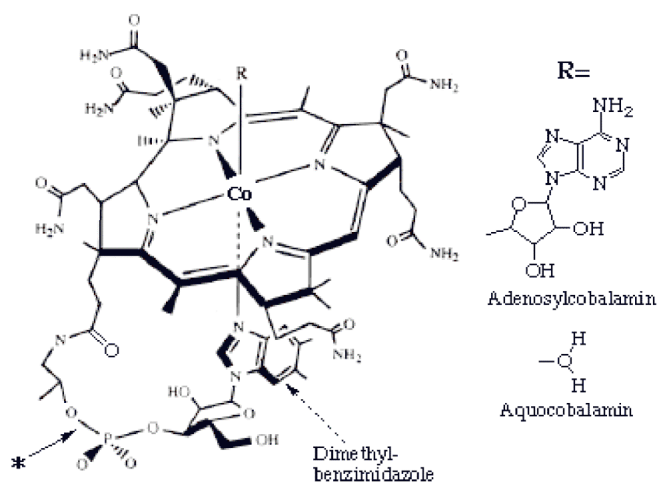
The catalytic module that we propose to use for this single protein system is the EutB protein from ethanolamine ammonia-lyase (EAL) from *Salmonella typhimurium*.<sup>5</sup> EAL consists of EutB (large subunit) and EutC (small subunit).<sup>6</sup> The EutB subunit

contains the robust  $(\beta\alpha)_8$  TIM-barrel fold,<sup>7</sup> which is a polypeptide-chain fold that is found in over 10% of proteins of known structure. In the TIM-barrel fold, 8  $\beta$ -strands form a closed barrel, with 8  $\alpha$ -helices surrounding them on the outside; the active site is located at the C-terminal end of the  $\beta$  barrel. Figure 1 shows (from a top view) how this closed barrel provides a protected inner region. In the closed  $\beta$  barrel, a network of hydrogen bonds between the  $\beta$  strands strengthens the structure. It is robust because of its ability to tolerate mutations, insertions, and replacements with little disruption to its stability. The EutB protein is well-suited for this project because it has multiple characteristics that will allow it to catalyze



**Figure 1.** Top view of the  $(\beta\alpha)_8$  TIM-barrel fold

the reduction of carbon dioxide ( $\text{CO}_2$ ), including its ability to bind cobalamin structures, space above the cobalt atom for axial ligands such as  $\text{CO}_2$ , and its ability to shield the reaction from other reactions that could interfere. The structure of a similar protein, EutB from *Listeria monocytogenes*, has recently been determined by X-ray crystallography.<sup>8</sup> The eventual goal of this project is to mutate the gene of the EAL protein to modify the active site for the reduction of  $\text{CO}_2$ . The cobalt cofactors that bind will act as the reducing agents for this reaction. The cofactors that will be used are the cobalamin and cobinamide centers.



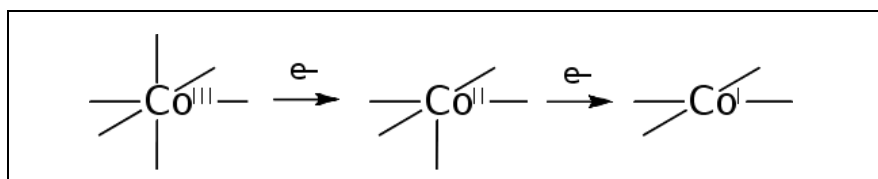
**Figure 2.** Structures of cobalamin cofactors

Figure 2 shows the structure of the cobalamin cofactor.<sup>5</sup> The cobinamide is obtained by cleaving the nucleotide loop at the position of the arrow in Figure 2. EutB is naturally able to bind adenosylcobalamin (known as coenzyme B<sub>12</sub>), which is one of the cobalamin cofactors. Cobalamin

contains a corrin ring macrocycle as its main feature, which contains four planar nitrogen atoms. These four nitrogen atoms are four of the six ligands which bind the cobalt atom in the cob(III)alamin state. Cobalamin also contains an upper ( $\beta$ ) axial ligand which differs between the different cobalamin derivatives and binds to the cobalt atom from above, as well as a lower ( $\alpha$ ) axial ligand (a “tail” that is linked to the cobalt macrocycle) called dimethylbenzimidazole (DMB) which binds to the cobalt atom from below. The cob(II)alamin state only has 5 ligands bound to cobalt (the four coplanar nitrogen atoms as well as the dimethylbenzimidazole (DMB)). In the cob(I)alamin state, both the upper and lower axial ligands are un-bound.

Each oxidation state

differs by one axial



**Figure 3.** Coordination of cobalt oxidation states

ligand, as shown in Figure 3. Cobalamin is referred to as “base-on” because of the presence of the dimethylbenzimidazole (DMB) axial ligand. The nucleotide loop can be chemically removed to form the “base-off” version of cobalamin, cobinamide. This “base-off” cobinamide is more easily reduced to the cobalt (I) state than cobalamin because of the absence of DMB, which is bound to cobalt in cob(II)alamin. The  $E_m$  from cob(II)inamide to cob(I)inamide is  $-0.74$  V, compared to the more negative  $-0.95$  V for cob(II)alamin to cob(I)alamin.<sup>9</sup> Although it is easier to reduce cob(II)inamide ( $E_m = -0.74$  V), the resulting cob(I)inamide is not as strong of a nucleophile as the cob(I)alamin. In the active site of the protein,  $\text{CO}_2$  is expected to bind to the fully reduced cob(I)alamin and undergo a two-electron, two-proton reduction reaction to form formate, as shown in Figure 4.

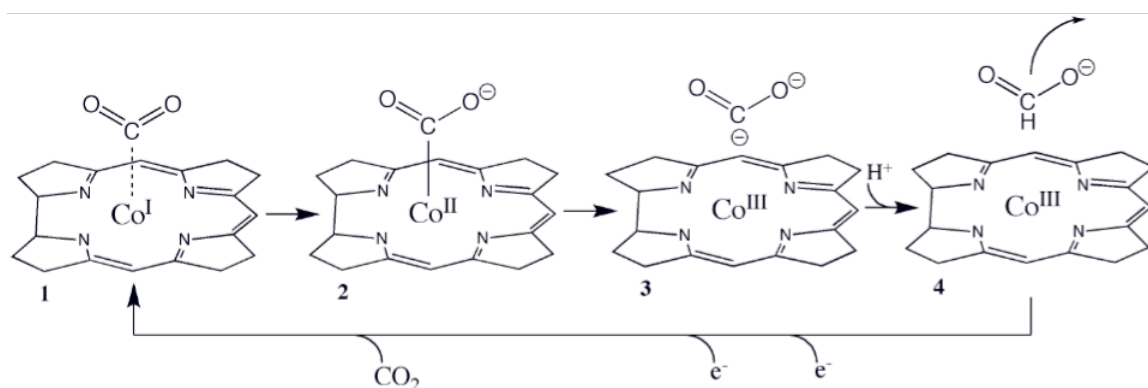


**Figure 4.** Target reaction between cob(I)alamin and  $\text{CO}_2$ , in the active site of EutB

In this project, the cobalamin and cobinamide cofactors are examined in a free solution system (outside of the protein environment). Ultraviolet (UV)/visible spectroscopy is used to characterize the cofactors in the absence and presence of carbon dioxide. This information is important for comparison with the studies of the enzyme-bound system, to investigate how they perform in the different environments, and to

determine how well the enzyme catalyzes the reaction. The three redox states of cobalamin and cobinamide, Co(III), Co(II), and Co(I), have distinct UV/visible spectra, and it is therefore possible to determine which species are present in solution. In order to reduce cobalamin to the Co(I) state, a strong chemical reducing agent must be used and the characteristic time factor ( $\tau$ ) for reduction is relatively long. In this project the focus is on the cobinamide compounds, which can be rapidly reduced all the way to the Co(I) state using the photo-activated reducing agent,<sup>10</sup> 5'-deazariboflavin (5'-DRF). A sacrificial electron donor (EDTA) is used to reduce the oxidized 5'-DRF.

## II. Experimental Procedures

### *Absorption Spectroscopy*

To measure absorption, a Shimadzu UV/visible 1601 spectrophotometer was used. The concentration of different oxidation states was calculated using Beer's Law. The spectrophotometer compares the intensity of the light that has passed through the sample to that of the initial light beam; the ratio of the two intensities ( $I/I_0$ ) is called the transmittance (T), and is used to define the absorbance (A):

$$A = -\log(T) \tag{1}$$

The samples were made anaerobic by sparging using nitrogen gas bubbling. The samples were placed in a cuvette with a sealable cap. Nitrogen gas was delivered into the cuvette by a needle inserted through a septum, and both  $N_2$  and oxygen ( $O_2$ ) gas left the sample through an exit needle. The septum re-sealed once the needle was removed, preventing oxygen from re-entering the sample. Nitrogen ( $N_2$ ) gas from an  $N_2$  tank was bubbled in through the needle for a time period of 15 minutes, after which the sample was deoxygenated.

### *Photolysis Studies*

To photolyse methylcobinamide (MeCbi), samples in cuvettes (vide supra) were placed 15 cm from a 300 W xenon lamp. The xenon lamp was allowed to warm up for exactly 30 seconds in all cases before it was turned on for photolysis. The samples were then

irradiated for 15 seconds. After irradiation, the samples were transferred to the UV/visible spectrometer for spectrum acquisition. If the experiment involved monitoring decay, a 1 hour time course with detection at 387nm was then performed immediately after the full spectrum; generally, the time taken from the initiation of photolysis until the 1 hour time course started was 1 minute and 25 seconds.

In the case of methylcobalamin (MeCbl), a 532nm laser was used to photolyze the sample with pulses of light for 1 minute and 30 seconds. The sample was moved up and down in the path of the laser so as to photolyze the entire volume.

#### *Preparation of MeCbi Samples*

A 0.5M MES (2-(*N*-morpholino)ethanesulfonic acid) solution was prepared for use in all of the MeCbi samples as well as in the MeCbl experiment, to buffer the pH. MES is a common buffering agent in biology and biochemistry, and has a  $pK_a$  of 6.15, and a buffer range of pH 5.5 to pH 6.7. This 0.5 M buffer solution was used to prepare a 100 mM MES and 1 mM ethylenediaminetetraacetic (EDTA) stock solution with a pH of 6.0. EDTA was used as the sacrificial electron donor for the MeCbi to Cob(I)inamide reduction experiments. MeCbi was added at a concentration of 50  $\mu$ M from a stock solution of MeCbi. When bicarbonate solution was to be added, the sample would be made anaerobic first by the nitrogen gas bubbling method. Once this was accomplished, the bicarbonate solution was injected in via syringe to the solution while it was kept under nitrogen gas pressure so that no oxygen would be able to enter. Once the solution was injected, the syringe was removed, and the nitrogen gas pressure was removed,

keeping the sample under positive pressure. For the 10 mM bicarbonate sample, a 0.5 M stock solution of sodium bicarbonate was added via syringe.

For samples that had 20 mM and 50 mM bicarbonate solution injected via syringe, the pH of the buffered solution was adjusted a pre-determined amount beforehand so that the final pH of buffered solution with bicarbonate added would be 6.0. For the 20mM bicarbonate sample, a 1 M stock solution of sodium bicarbonate was made. A 1:3 solution of HCl/water was diluted 10x; 15  $\mu$ L of this diluted HCl was then added for every 20  $\mu$ L of 1 M bicarbonate solution that was to be added via syringe. The 15  $\mu$ L of HCl lowered the pH by 0.3, and the 20  $\mu$ L of 1 M bicarbonate solution raised it by 0.3, bringing the pH back to the initial value of 6.0. For the 50 mM bicarbonate sample, a 1 M was also used as the stock, but the volume of solution added via syringe was increased by 2.5 times. For the 50 mM sample, 65  $\mu$ L of 10x diluted 1:3 HCl/water solution was added for every 50  $\mu$ L of 1 M bicarbonate solution to be added; this resulted in a final pH that returned to 6.0.

MeCbi was taken from a stock solution and added to a 100 mM MES/ 1mM EDTA buffered solution into a 4mL anaerobic cuvette. The solution was made anaerobic by the nitrogen gas bubbling method; nitrogen gas was bubbled through the solution for 15 minutes. Once anaerobic, a spectrum was taken of the (III) oxidation state MeCbi solution; it was then exposed to a 300 W xenon lamp for 15 seconds of irradiation, and another spectrum was taken of the cob(II)inamide created by photolysis. This process was repeated for another non-anaerobic MeCbi solution, and photolysis in this case generated AquoCbi. Cob(I)inamide was generated by creating an anaerobic solution of MeCbi in the 100mM MES/1mM EDTA buffer solution with the addition of 5 $\mu$ M 5'

Deazariboflavin (5'DRF) to reduce the MeCbi to the Co(I) state. The molarities were calculated by comparing the spectra of MeCbi at pH of 7.5 to that of the same concentration at pH of 6.0. Once these were determined to be the same, the concentration at 6.0 was used to determine the new extinction coefficients for the rest of the cobinamide compounds at 6.0, which were similar to the pH 7.5 counterparts.

*Fitting of the cob(I)inamide decay kinetics*

The cob(I)inamide decay reaction was measured by the loss of absorbance at 387 nm ( $A_{387}$ ). The absorbance *versus* time plot was fitted by using the single exponential plus constant function, as follows:

$$A_{387} = A_1 e^{-t/\tau} + C \quad (2)$$

where  $A_1$  is the amplitude of the exponential decay,  $C$  is the constant amplitude, and  $\tau$  is the time constant. The fits were performed by using MATLAB (Mathworks, Novi, MI).

### III. Results

#### *Absorption spectra of different cobalamin and cobinamide redox states*

The UV/visible absorption spectra for three different cobalamin compounds are shown in Figure 5. Aquocobalamin (AquoCbl) was generated by photolysis of MeCbl in aerobic solution. Cob(II)alamin was generated by photolysis of MeCbl under anaerobic conditions. MeCbl and AquoCbl are in the Co(III) redox state. The visible absorption maximum for MeCbl is located at 525 nm, while that of cob(II)alamin is at a shorter wavelength of 470 nm. AquoCbl also shows a long wavelength peak, but the large characteristic peak of AquoCbl is at 350 nm, and clearly separated from those of MeCbl and cob(II)alamin. The spectra show that it is possible to determine the different redox and coordination states of these cobalamins by using UV/visible absorption spectrophotometry.

Figure 6 shows the absorption spectra for four different cobinamide compounds, in different cobalt redox states. All four of the compounds were derived from MeCbi, in which cobalt is in the Co(III) state, which has a characteristic visible absorption peak at 465 nm. When the MeCbi solution was made anaerobic and then photolyzed, the result was cob(II)inamide, which has a slightly different spectrum, relative to the MeCbi, with a distinguishing peak in the UV region at 310 nm. With the addition of 5'-DRF, followed by illumination, the cob(II)inamide was photo-reduced to cob(I)inamide. Cob(I)inamide has a distinctive large peak at 387 nm, and relatively small absorption in the visible region. When the sample of MeCbi is not made anaerobic, photolysis yielded aquocobinamide (AquoCbi), which has a strong characteristic absorption at 350 nm. The unique characteristic peaks of the different cobinamide redox states allow us to determine

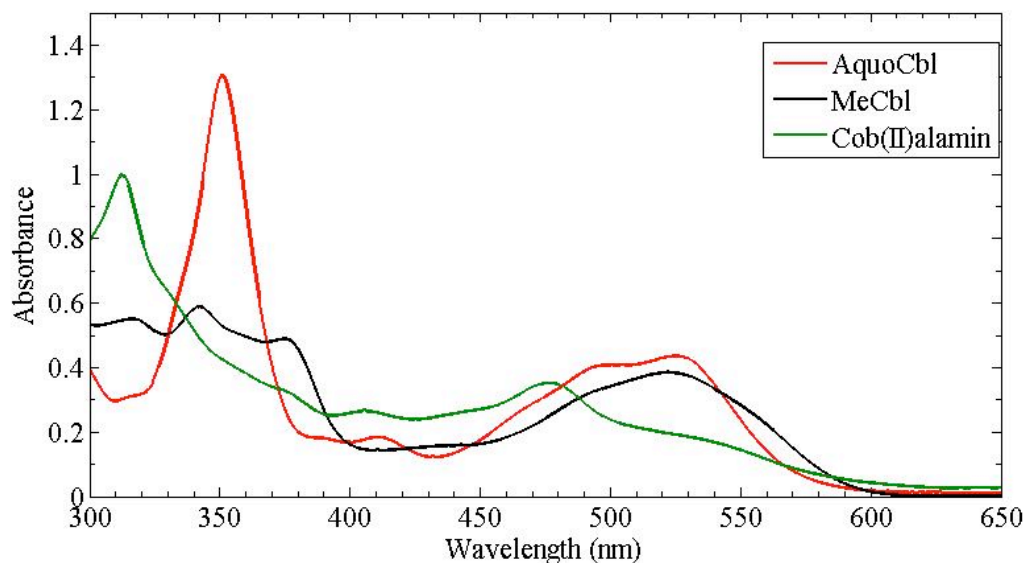


**Figure 5.** UV/visible absorption spectra of cobalamin compounds in aqueous solution at room temperature. The cobalamin concentrations are  $50 \mu\text{M}$ , in  $10 \text{ mM}$  MES, pH 6.0 (MeCbl and cob(II)alamin) and pure water (AquoCbl).

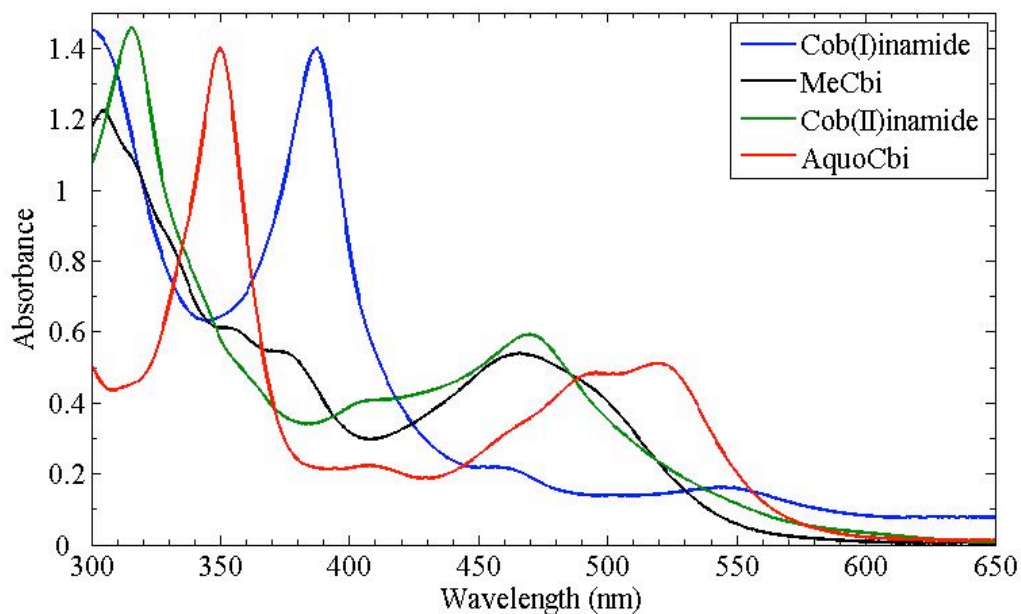


**Figure 6.** UV/visible absorption spectra of cobinamide compounds in aqueous solution at room temperature. The cobinamide concentrations are  $51.0 \mu\text{M}$ , in  $100 \text{ mM}$  MES and  $1 \text{ mM}$  EDTA (pH 6.0).

their relative concentrations in solution, and to monitor the change from one redox state to the next by using UV/visible absorption spectroscopy.

*Assay for the determination of oxygen concentration in the samples*

An assay was developed, in which the photolysis of MeCbl, and the subsequent reaction of the cob(II)alamin photoproduct with oxygen ( $O_2$ ) to form AquoCbl (Co(III)), was used to quantify the oxygen content in the samples. This was important, because it was necessary to determine the amount of oxygen carried over into the sample from the stock solutions, so that the amount of oxygen, and the effect of any oxygen on the photolysis products in the experiments, could be characterized. The oxygen assay was also used to assess the possible leakage of oxygen into our samples. Figure 7 (top) shows the UV/visible spectrum of a 50  $\mu$ M methylcobalamin solution, that was first made anaerobic by the nitrogen gas bubbling technique, and then photolyzed using the 532 nm laser for 90 s. In this solution, nothing was added before photolysis. Figure 7 (bottom) shows the UV/visible spectrum of a MeCbl solution of the same concentration, except to this sample, 10 mM of bicarbonate was added via syringe (80  $\mu$ L of 0.5 M bicarbonate solution) after the solution was made anaerobic. Once the bicarbonate was added, the sample was photolysed in the same manner as the first sample. Comparing the two spectra, the difference in absorbance at 350 nm (Figure 7, arrow) reveals the presence of AquoCbl. The AquoCbl was formed by reaction of the cob(II)alamin photoproduct with oxygen. The height of the 350 nm peak can be used to calculate the amount of oxygen added through the bicarbonate solution. The difference in concentration of AquoCbl is 2  $\mu$ M. The predicted concentration of oxygen in the sample, based on the solubility of oxygen in water at room temperature (250  $\mu$ M) and the volume of the aliquot transferred to the sample, is 2  $\mu$ M. Therefore, the MeCbl photolysis method is useful for quantifying

trace oxygen contents in the experiments. The carry-over concentration of 2  $\mu\text{M}$  was not significant enough to perturb the  $\text{CO}_2$  reduction experiments. In addition, by using the assay, we found that the samples were not perturbed by oxygen leaks, on the time scales (up to hours) of the experiments.

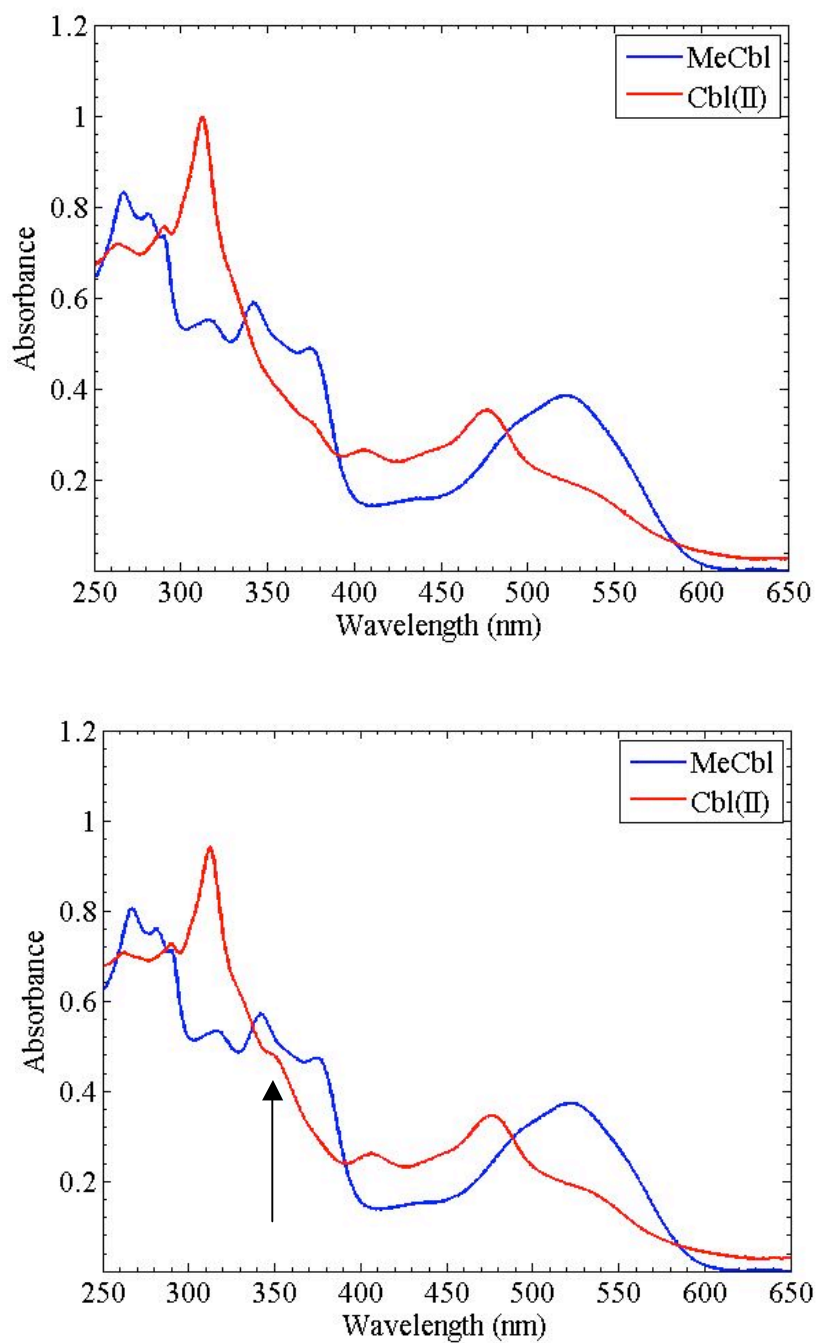


**Figure 7.** (Above) Ultraviolet/visible spectra of MeCbl and photolysis to Cbl(II) without bicarbonate added, (Below) Ultraviolet/visible spectra of MeCbl and photolysis to Cbl(II) with bicarbonate added

*Reaction of cob(I)inamide in aqueous solution at pH 6.0*

The reaction of cob(I)inamide in anaerobic aqueous solution at pH 6.0 was addressed as a control for the reaction of cob(I)inamide with solutions containing CO<sub>2</sub>. The pH of 6.0 was chosen, because the CO<sub>2</sub> concentration increases with decreasing pH. Figure 8 (Left and Right) are the plots for the decay of cob(I)inamide with water added (control for the addition of the bicarbonate solution, in the experiments with CO<sub>2</sub>) and with nothing added (control for effect of carry-over oxygen from the bicarbonate stock; in this control, not oxygen is delivered to the sample), respectively, measured at 387 nm, which is the characteristic peak of cob(I)inamide. Water was added via syringe in a volume of 80 μL, after N<sub>2</sub> bubbling of the sample, and before photolysis. Decreasing absorbance at 387 nm signals a decrease in cob(I)inamide concentration. Spectra taken during the decay (separate experiments), and at the end of the experiment presented showed that the cob(I)inamide decrease was associated with an increase in cob(II)inamide concentration. No Co(III)-cobinamide species were detected.

The decay data were fitted to a single exponential plus constant function. The average fitting parameters for the decay amplitude, the decay time constant (characteristic, or 1/e time), and the constant amplitude are presented in Table 1. The decay time constants for the water-added (9.1 ±0.6 min) and nothing-added (10.1 ±0.5 min) were comparable. The results show that cob(I)inamide decays on the approximately 10 min time scale, in the absence of any added reactant. Therefore, this background reaction will compete with the desired reaction of cob(I)inamide with added CO<sub>2</sub>.

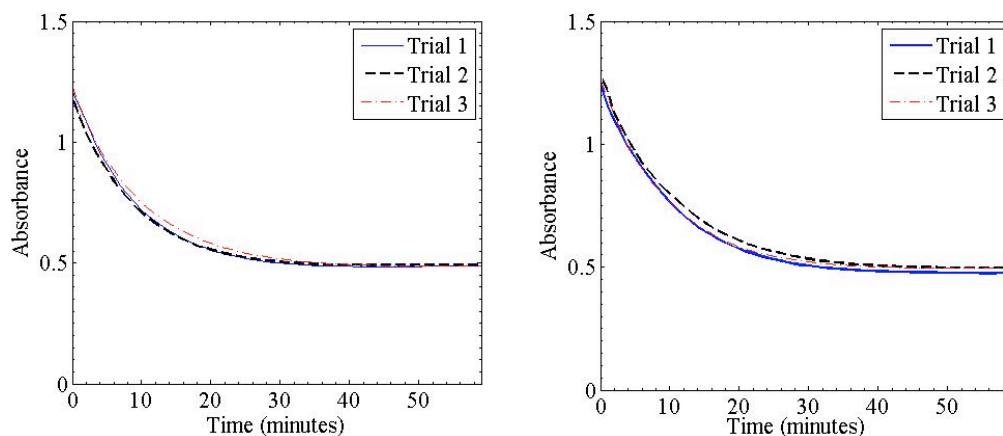


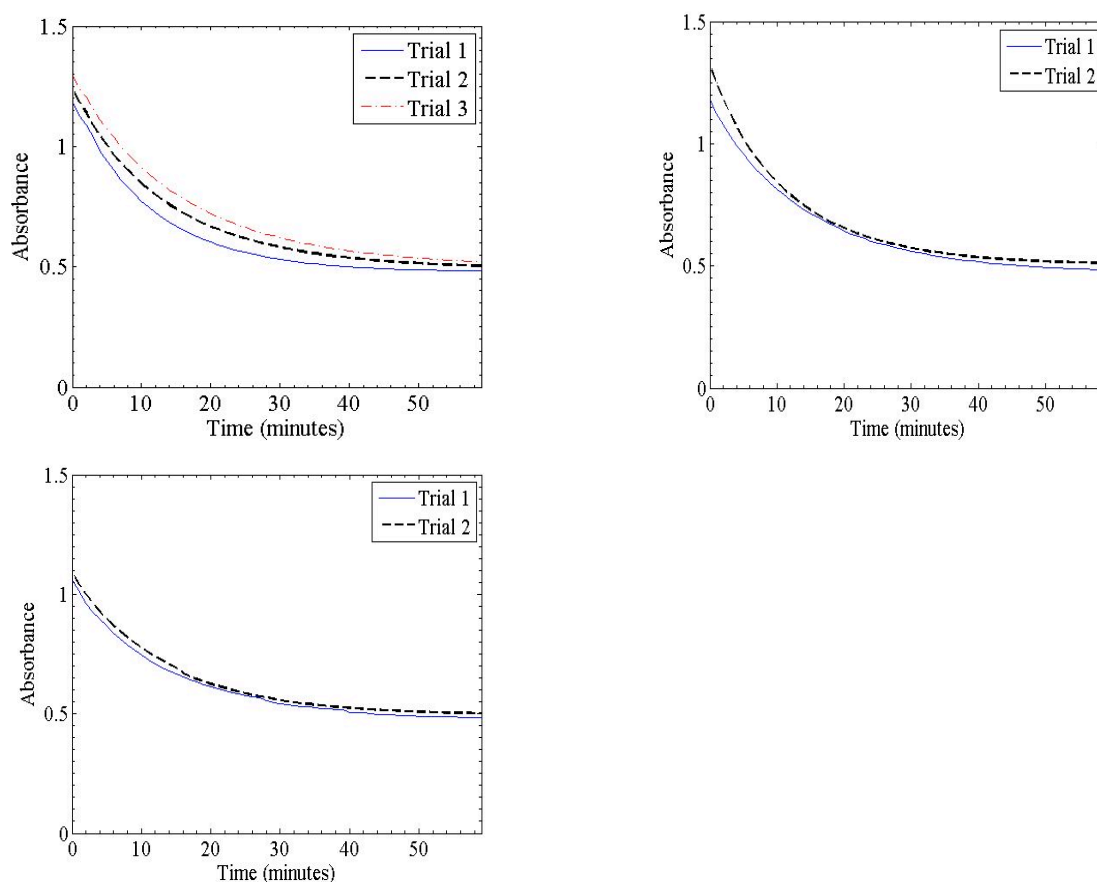
**Figure 8.** Reaction of photo-generated cob(I)inamide in aqueous solution at pH 6.0. Left: Water was added to the sample, as a control for the addition of bicarbonate solution. Right: No additions to the sample. The absorbance was detected at 387 nm, which corresponds to the UV absorption peak of cob(I)inamide.

#### *Reaction of cob(I)inamide with CO<sub>2</sub> in aqueous solution at pH 6.0*

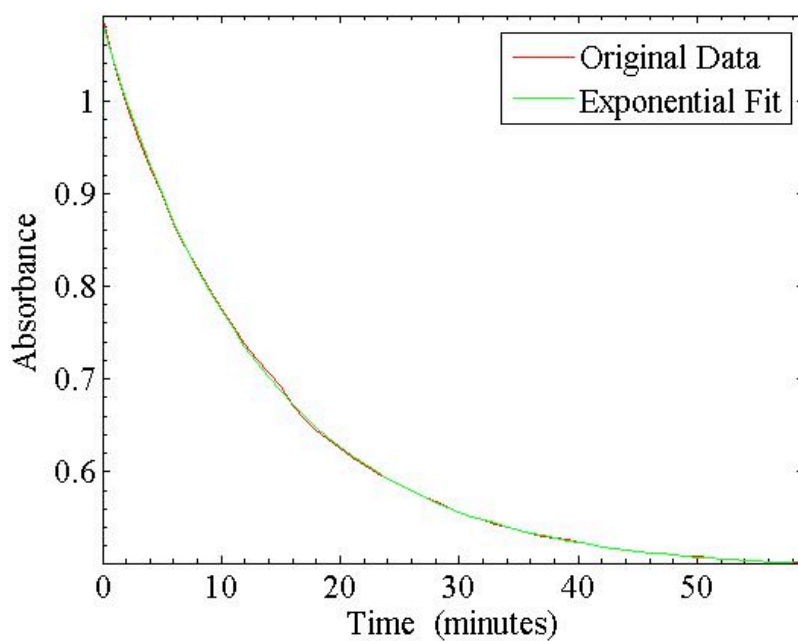
The reaction of cob(I)inamide with CO<sub>2</sub> in anaerobic aqueous solution at pH 6.0 was addressed in solutions that contained different bicarbonate concentrations. As stated above, the pH of 6.0 was chosen, because the CO<sub>2</sub> concentration increases with decreasing pH. Figure 9 shows the plots of the data for the cob(I)inamide decay in the presence of bicarbonate, at final concentrations of 10 mM, 20 mM, and 50 mM. The same volume of 80 μL was added for the 10 mM and 20 mM trials. However, for the 50 mM trials, the amount of bicarbonate solution added was increased by 2.5-fold, owing to the restrictions of solubility of sodium bicarbonate. UV/visible spectra obtained following the decay of the samples, again showed that the reaction product was cob(II)inamide. No Co(III) species were detected.

Table 1 shows that the single exponential plus constant function also provides an excellent fit to the data for the decays of cob(I)inamide in the presence of bicarbonate

(CO<sub>2</sub>), which are shown in Figure 9. The average time constant values are  $13.4 \pm 2.0$ ,  $12.7 \pm 1.7$ , and  $13.5 \pm 0.2$  min for the 10 mM, 20 mM and 50 mM bicarbonate samples, respectively. These values are all significantly larger than the time constants for the control decays of  $9.1 \pm 0.6$  min (water added) and  $10.1 \pm 0.5$  min (nothing added) (Figure 8, Table 1). This was unexpected, because our hypothesis was that added CO<sub>2</sub> would react with cob(I)inamide, and make the decay more rapid. As explained in more detail in the Discussion, our interpretation is that the CO<sub>2</sub> interacts weakly with cob(I)inamide, to produce the effect of longer decay time constant.



**Figure 9.** Reaction of photo-generated cob(I)inamide in aqueous solution at pH 6.0 in the presence of different concentrations of bicarbonate. Top, left: 10 mM Bicarbonate added. Top, right: 20 mM Bicarbonate added. Bottom: 50 mM Bicarbonate added. The absorbance was detected at 387 nm, which corresponds to the UV absorption peak of cob(I)inamide.



**Figure 10.** Original data from Trial 2 of the 50 mM bicarbonate experiment, with the exponential fit curve overlaid.

Table 1 presents the various coefficients and constants for the monoexponential fits to the data of Figures 8 and 9. The  $A_1$  constant represents the amplitude, the  $t_1$  constant is the time constant,  $\tau$ , and the  $r$  parameter represents how good of a fit the exponential curve is to the actual data. Figure 10 provides an example exponential fit to the data.

**Table 1.** Monoexponential fit constants for the data of Figure 8 and 9

|                   |           |              |
|-------------------|-----------|--------------|
| Nothing Added     | Average   | Standard Dev |
| $A_I$             | 7.757E-01 | 5.200E-03    |
| $\tau$            | 1.006E+01 | 5.209E-01    |
| $C$               | 4.831E-01 | 1.299E-02    |
| $res$             | 8.473E-04 | 2.097E-04    |
| $r$               | 9.998E-01 | 4.431E-05    |
| Water Added       | Average   | Standard Dev |
| $A_I$             | 7.292E-01 | 2.657E-02    |
| $\tau$            | 9.086E+00 | 6.342E-01    |
| $C$               | 4.830E-01 | 3.904E-03    |
| $res$             | 6.584E-04 | 3.804E-04    |
| $r$               | 9.998E-01 | 9.511E-05    |
| Bicarbonate 10 mM | Average   | Standard Dev |
| $A_I$             | 7.460E-01 | 3.611E-02    |
| $\tau$            | 1.336E+01 | 1.958E+00    |
| $C$               | 4.947E-01 | 1.464E-02    |
| $res$             | 4.099E-04 | 1.099E-04    |
| $r$               | 9.999E-01 | 2.295E-05    |
| Bicarbonate 20 mM | Average   | Standard Dev |
| $A_I$             | 7.453E-01 | 7.269E-02    |
| $\tau$            | 1.274E+01 | 1.711E+00    |
| $C$               | 4.935E-01 | 2.404E-02    |
| $res$             | 6.485E-04 | 3.024E-04    |
| $r$               | 9.999E-01 | 7.071E-05    |
| Bicarbonate 50 mM | Average   | Standard Dev |
| $A_I$             | 6.273E-01 | 5.374E-02    |
| $\tau$            | 1.352E+01 | 1.626E-01    |
| $C$               | 4.865E-01 | 1.061E-02    |
| $res$             | 8.029E-04 | 7.695E-04    |
| $r$               | 9.997E-01 | 2.828E-04    |

#### **IV. Discussion**

##### *Establishment of Reliability and Reproducibility in Cobalamin/ Cobinamide – CO<sub>2</sub> Reactivity Measurements*

One of the challenges of characterizing the interaction and reaction between CO<sub>2</sub> and the cob(I)inamide was to make the experiment both reproducible and reliable. Before the final method that was developed in this work was arrived at, other methods were tried, which produced results that were not reproducible because of the variations in the experiment from trial to trial. These variations were usually caused by oxygen being able to enter the sample at various points during the experiment, or were caused by the concentration of CO<sub>2</sub> not being constant. The concentration of CO<sub>2</sub> is heavily dependent on the pH of the solution, so it was important to make sure that the solution was well buffered and that the initial and final pH values were known.

Before proceeding with the final experiment, it was necessary to first determine exactly how much oxygen would be added along with the aerobic bicarbonate. To do this, we developed an assay to sensitively detect the amount of oxygen present in the sample solution which was based upon how much photo-generated cob(II)alamin reacted with oxygen and formed AquoCbl. This assay also detected any oxygen that would have leaked into the sample container (cuvette) after the solution was injected. Oxygen contamination was a concern, because the sample was agitated into the overhead space in order to mix, before the final spectrum was taken.

In order to make sure that the concentration of CO<sub>2</sub> was constant throughout all of the experiment, the pH was also carefully established, and then held constant. This was done by adjusting the pH of the buffer before addition of the bicarbonate, which is able to

change the pH in the region of interest. Because of this, the adverse factors that contributed to variations in the background rate of reaction of protons with cob(I)inamide were eliminated. Effects of pH variation on the absorbance of the cobalt complexes were also eliminated.

### *Dihydrogen formation*

In our system, which is in aqueous solution, once the cob(I)inamide is formed it is subject to reaction with protons in solution. The following equations have been proposed for the process by which the protonation of the Co(I) state and formation of dihydrogen (H<sub>2</sub>) proceeds:<sup>11, 12</sup>



First, the cob(I)inamide is protonated to form the  $[\text{Co(III)H}^-]^{2+}$  species which is formally a Co(III) - hydride.<sup>10</sup> The hydride can then be protonated to release H<sub>2</sub>, which leads to formation of Co(II). Alternatively, the hydride can react with another hydride in solution to eliminate H<sub>2</sub>.<sup>12</sup> As can be seen in Figure 8, the photogenerated cob(I)inamide decays to cob(II)inamide in the presence of protic solution (water). Thus, the observed cob(I)inamide decay is consistent with the above reaction mechanisms.

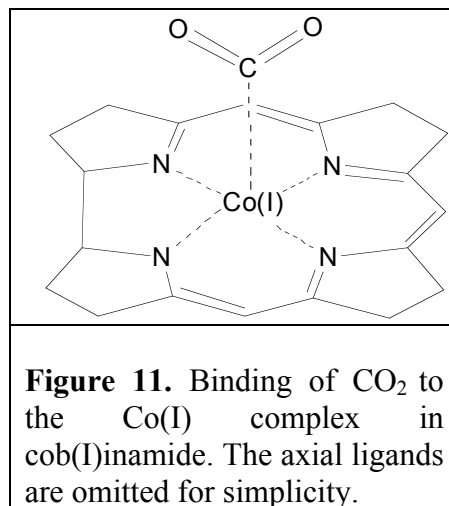
A similar experiment was performed by Ogata et al. in a nominally aprotic organic solvent (acetonitrile/methanol), instead of an aqueous solvent.<sup>11</sup> When they introduced CO<sub>2</sub> into their system, the interaction of the CO<sub>2</sub> with the Co(I) complex increased the rate of decay to the Co(II) state. In the absence of water, there are no readily available protons, and therefore, the Co(I) state is much more stable in the absence of CO<sub>2</sub>. They found that the rate constant of the decay of Co(I) increased steadily as the concentration of CO<sub>2</sub> was increased. The apparent first order rate constant for the reaction was  $6.4 \times 10^4 \text{ s}^{-1}$ .

In our system, we found that the presence of CO<sub>2</sub> resulted in a decrease in the rate of decay of cob(I)inamide. Table 1 shows the time constants generated from the exponential fits to the data in Figure 8 and Figure 9. The time constants for the “Nothing Added” and “Water Added” control experiments are very similar, while those from the 10 mM, 20 mM, and 50 mM bicarbonate experiments show a decrease in the rate of cob(I)inamide decay. While we were not able to detect the CO<sub>2</sub> by using UV/visible spectroscopy, it could be that a lower temperature is required to increase coordination by the solution of the CO<sub>2</sub> – cob(I)inamide complex and make the absorption more noticeable in the spectrum, as reported by Ogata et al.<sup>11</sup>

*CO<sub>2</sub> binding interaction with cob(I)inamide*

We propose that increasing time constants for decay of cob(I)inamide with increasing CO<sub>2</sub> concentration is caused by the binding of CO<sub>2</sub> to cob(I)inamide, which stabilizes the complex and prevents competing proton reduction reactions from occurring.

CO<sub>2</sub> is naturally a linear molecule. Because of the two electronegative oxygen atoms that are bound to the carbon atom, the electron distribution results in a slight positive charge on the carbon. This slight electrophilic property of the carbon atom in CO<sub>2</sub> allows it to bind to a nucleophilic metal center (one with high electron density) in the case that there is an



available binding site. There are three main modes in which a CO<sub>2</sub> molecule can bind to a metal center, termed  $\eta^1$ ,  $\eta^2$ -side-on, and  $\eta^1$ -O-end-on.<sup>13</sup> In the  $\eta^1$  mode, the metal interacts with the  $\pi^*$  molecular orbital of CO<sub>2</sub>, creating a binding interaction. This mode results in a modification of the natural shape of CO<sub>2</sub> to a bent shape.

Figure 11 shows the proposed complex of cob(I)inamide and CO<sub>2</sub>. The CO<sub>2</sub> occupies the upper axial ligand position, preventing a solvent molecule from entering the region and transferring a proton to the complex. According to the results, an increased concentration of CO<sub>2</sub> promotes increased binding and a slowed decay rate.



Equation 6 shows a proposed reaction mechanism, in which the bound CO<sub>2</sub> could be reduced to carbon monoxide (CO). Other proposed mechanisms are for CO<sub>2</sub> binding to the Co(I) state, followed by reduction and protonation to form formate. In this reaction, a vacant coordination site would allow cobalt to form a bond with oxygen from the already bound CO<sub>2</sub> molecule. This oxygen would be protonated, allowing for the cleavage of the C-O bond and the release of CO (Dubois and Dubois).

For the type of binding interaction proposed, we would expect to see a hyperbolic curve when the time constant is plotted against the concentration of bicarbonate. This is because, for an increasing time constant, we would expect for more CO<sub>2</sub> to be bound at any given time (K<sub>off</sub> to be lower).

$$K_{\text{diss}} = \frac{K_{\text{off}}[\text{CO}_2]}{K_{\text{off}}} \quad (7)$$

If the curve were to be a linear increase in time constant, one explanation could be a solution interaction (activity effect). When we add bicarbonate, it increases the negative charges present in solution. These are able to shield protons from cob(I)inamide. In our data, because of the relatively high standard deviation, we cannot tell which of these is the mechanism of action. Further experiments are needed in the range between 0 and 10 mM of bicarbonate concentration to determine the character of this curve.

#### *Future Experiments and Outlook*

Although UV/visible spectral changes in the cob(I)inamide from interaction with CO<sub>2</sub> could not be resolved, infrared (IR) spectroscopy could be used to detect CO<sub>2</sub>

binding to cob(I)inamide. The IR absorption of CO<sub>2</sub> occurs in a region of low absorption by water and solution components, and shifts in the peak would show CO<sub>2</sub> binding. In addition, lowered temperature favors gas binding to metals. Binding and reactivity assays in the recently developed cryosolvent system will be used to further address this. Ultimately, the proton reduction reaction is one that competes with the binding of CO<sub>2</sub> and reduction of CO<sub>2</sub> and is one that will have to be excluded in order for the binding and eventual reduction of CO<sub>2</sub> to take place with high yields. This exclusion of the competing reaction will happen in the protein active site, allowing the cofactors to operate in a shielded environment. The results of this project, highlighting the effects of the proton interactions, point to the need for the protein system in an aqueous environment.

## V. References

1. Gray, H. B., Powering the planet with solar fuel. *Nature Chemistry* **2009**, *1*, 7.
2. Lewis, N. S.; Nocera, D. G., Powering the planet: Chemical challenges in solar energy utilization. *Proc. Natl. Acad. Sci.* **2006**, *103* (43), 15729-15735.
3. Ellis, R. J., The most abundant protein in the world. *TIBS* **1979**, *4*, 241-244.
4. Tcherkez, G. G. B.; Farquhar, G. D.; Andrews, T. J., Despite slow catalysis and confused substrate specificity, all ribulose biphosphate carboxylases may be nearly perfectly optimized. *P Natl Acad Sci USA* **2006**, *103* (19), 7246-7251.
5. Brown, K., Chemistry and Enzymology of Vitamin B12. *Chem. Rev.* **2005**, *105*, 2075-2149.
6. Sun, L.; Warncke, K., Comparative model of EutB from coenzyme B12-dependent ethanolamine ammonia-lyase reveals a b8a8, TIM-barrel fold and radical catalytic site structural features. *Proteins: Structure, Function, and Bioinformatics* **2006**, *64* (2), 308-319.
7. Gerlt, J. A.; Raushel, F. M., Evolution of function in  $(\beta/\alpha)_8$ -barrel enzymes. *Curr. Op. Chem. Biol.* **2003**, *7* (252-264).
8. Joint\_Center\_for\_Structural\_Genomics, Crystal structure of ethanolamine ammonia-lyase heavy chain (YP\_013784.1) from *Listeria monocytogenes* 4b F2365 at 2.15 Å resolution. **2007**, *10.2210/pdb2qez/pdb*.
9. Lexa, D.; Saveant, J. M., The Electrochemistry of Vitamin-B12. *Accounts Chem Res* **1983**, *16* (7), 235-243.

10. Massey, V.; Hemmerich, P., Photoreduction of Flavoproteins and Other Biological Compounds Catalyzed by De-Aza-Flavins. *Biochemistry-Us* **1978**, *17* (1), 9-16.
11. Ogata, T.; Yanagida, S.; Brunschwig, B. S.; Fujita, E., Mechanistic and Kinetic Studies of Cobalt Macrocycles in a Photochemical CO<sub>2</sub> Reduction System: Evidence of Co-CO<sub>2</sub> Adducts as Intermediates. *J. Am. Chem. Soc.* **1995**, *117* (25), 6708-16.
12. Dempsey, J.; Brunschwig, B. S.; Winkler, J. R.; Gray, H. B., Hydrogen evolution catalyzed by cobaloximes. *Acc. Chem. Res.* **2009**, *42* (12), 1995-2004.
13. Gibson, D. H., The organometallic chemistry of carbon dioxide. *Chemical Reviews* **1996**, *96*, 2063-2095.